Innovative frequency and voltage controller for AC microgrid

Xuan Hoa Thi Pham, Hai Van Tran
Department of Electrical and Electronic Engineering, Ho Chi Minh City University of Industry and Trade, Ho Chi Minh City, Vietnam

Article Info

Article history:

Received Nov 10, 2024
Revised Mar 18, 2026
Accepted Apr 23, 2026

Keywords:

Control microgrid
Frequency control
Fuzzy logic
Power sharing
Voltage control

ABSTRACT

This paper designs a power controller for power converters using fuzzy logic. The proposed controller will automatically adjust the frequency and voltage when the load changes to improve the power quality of the microgrid. Besides, the controller can realize accurate power sharing among the power converters in the microgrid, thereby suppressing the circulating current between the inverters. Furthermore, to ensure the control system operates stably and accurately during voltage and frequency adjustments, this paper employs a sliding-mode controller rather than a conventional proportional-integral controller. The proposed control method has a voltage deviation from the rated value when the load changes in the range of 1.5 Volts to 2.7 volts, and a frequency deviation from the rated value when the load changes in the range of 0.2 to 0.4 Hz. The accuracy of reactive power division is 100%. The proposed controller is simulated using MATLAB/ Simulink software, and the results obtained from the simulation have verified the effectiveness of the proposed method.

Corresponding Author:

Xuan Hoa Thi Pham
Department of Electrical and Electronic Engineering, Ho Chi Minh City University of Industry and Trade
Ho Chi Minh City, Vietnam
Email: hoaptx@huit.edu.vn

1. INTRODUCTION

Microgrids include distributed energy sources such as wind power, and solar power. Microgrids need to use inverters to supply AC power to AC loads and connect to the grid. Power transmission in microgrid is highly efficient when inverters are connected in parallel [1], [2]. Currently, the issue of controlling parallel-connected inverters in microgrid is attracting considerable attention from researchers both domestically and internationally, particularly research into improving controllers to enhance accuracy in power distribution and eliminate balancing currents running in the inverters. However, these methods have not yet been applied to reduce voltage and frequency deviations in small power grids [3], [4]. Based on the power characteristics of the inverters, these studies have used the slope characteristics of Droop to control power distribution between parallel-connected inverters. According to the slope characteristics of the Droop, active power shifts with frequency, and reactive power shifts with voltage. Therefore, researchers have relied on the slope factor of the Droop to realize sharing power for parallel-connected inverters. However, the power sharing for inverters by the droop method will cause significant frequency and voltage deviations. As the load's power demand increases, the frequency and voltage of the power grid decrease significantly [3], [4]. Researchers have presented methods to improve slope characteristics to enhance power-sharing efficiency. However, the improvements are not aimed at reducing voltage and frequency deviations to improve power quality [5]-[7]. In addition, some research works [8]-[13] have proposed methods to improve reliability and save costs during microgrid operation. These studies have proposed smart protection schemes for microgrids and fault identification methods during operation, some adaptive and reliable protection schemes to detect faults and isolate faults quickly based on weather.

Fuzzy logic is increasingly used in microgrid power control due to its ability to handle complex non-linear systems and uncertainties, providing a robust and adaptive approach to energy management. Fuzzy logic controllers (FLCs) are particularly well-suited to microgrids because they can optimize energy distribution, manage variability from renewable energy sources, and maintain stable operation under a wide range of conditions. FLCs are used to manage the flow of power between different sources such as solar, wind, batteries, diesel generators, and loads. FLC uses fuzzy rules based on linguistic variables "high", "low", and "medium" to determine the optimal power allocation, taking into account factors such as renewable energy availability, battery state of charge (SOC), and load demand. FLC is robust to uncertainties and disturbances, suitable for practical microgrid applications, FLC can adapt to changing conditions and optimize performance based on real-time feedback, FLC provides smooth control response, simple design, relatively few parameters and rules, making them easier to deploy than some other control strategies. In summary, fuzzy logic plays an important role in power control for microgrids. It provides a powerful and flexible approach to managing energy resources, ensuring stability and optimizing performance under different operating conditions. Currently, there have been many research works applying FLC to microgrid control. Research [14], [15] have addressed the improvement of the controller for the photovoltaic system connected to the battery energy storage system, under the conditions of solar radiation, temperature, non-linear conditions, and load. Research [16], [17] have proposed an optimal DC bus voltage regulation method using adaptive FLC and a new monitoring power management strategy for PV systems. The goal is to maintain a stable power flow in the system. Studies [18], [19] have proposed an energy management method for microgrids based on fuzzy logic and data analysis monitoring to adjust the optimal power of objects in the microgrid. However, most of the research is only applied to the DC subgrid of the microgrid; there are not many studies applied to the AC grid of the microgrid.

This article proposes a controller for inverters using fuzzy logic to stably adjust the voltage and frequency for the AC microgrid. The proposed controller will offer the following benefits: The proposed controller can automatically adjust the frequency and voltage of the microgrid. In addition, this control method also maximizes the power distribution efficiency for the inverters. Therefore, this controller will keep the voltage and frequency in the microgrid stable, only varying within the permissible range, ensure the accuracy of power sharing between inverters, and also eliminate the balancing current flowing in the inverters. The proposed controller is applied to power control for a common microgrid with the configuration in Figure 1 [20]-[23]. This configuration involves interconnected renewable energy sources on a DC bus. This type of configuration reduces the number of inverters, and the system can operate flexibly depending on the control method. This article focuses on control methods to maintain voltage and frequency stability, minimize frequency and voltage deviation of the microgrid, and share the power output precisely with the inverters. Therefore, the renewable energy sources concentrated on the DC bus in Figure 1 are assumed to always provide sufficient power to the loads.

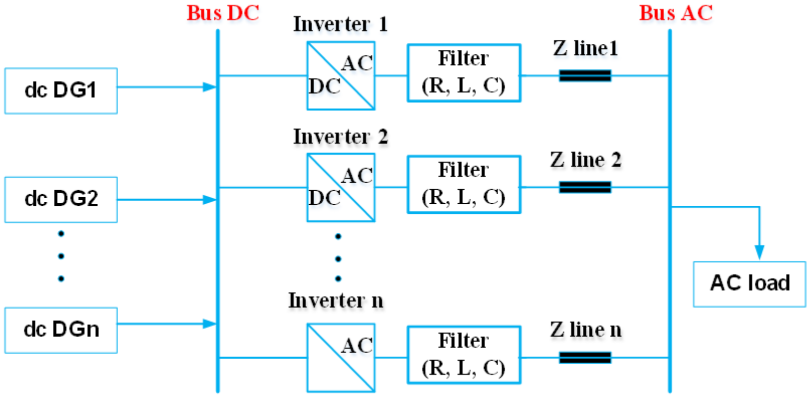

Figure 1. Configuration of a common standalone microgrid

2. METHOD

The focus of the proposed control method is: i) maintaining voltage and frequency stability, minimizing frequency and voltage deviations of the microgrid, ii) accurately distributing power to the inverters to eliminate circulating current and noise currents generated when the inverter output parameters are inconsistent. The proposed control method is implemented as follows:

- First, based on the theoretical basis of the conventional Droop method for power sharing among inverters. Studies [3]-[5] presented the droop method for low-voltage networks, the droop method for medium-voltage networks was presented in studies [6]-[8], and studies [9]-[13] presented the droop method for distribution networks from low to medium voltage to expand the application scope of the droop method. The theoretical basis of the conventional droop method is presented in section 2.1.
- Next, the disadvantages of the conventional Droop method presented in section 2.1 are analysed as follows: i) it is impossible to accurately share power when the output parameters of the inverter are inconsistent, leading to the appearance of circulating current and noise current that damage the inverter; ii) when the load increases or decreases sharply, it will cause very large frequency and voltage deviations, which may exceed the permissible range. This content is presented in section 2.2.
- Finally, the paper proposes a method to improve the conventional Droop controller by: i) using a fuzzy logic controller in combination with the conventional Droop controller. The fuzzy controller will automatically adjust the slip coefficient to shift the Droop graph. The proposed controller will result in: accurate power sharing among the inverters, thereby eliminating the cyclic current; and reduced frequency and voltage deviations of the microgrid when the load changes. This is presented in section 2.3. ii) On the other hand, to maintain the stability of the control system for the microgrid, the paper also uses a sliding mode controller (SMC) instead of the conventional proportional-integrating (PI) controller. The SMC will stabilize the current and voltage at the inverter output. iii) Simulation results in section 3 will demonstrate the suitability of the proposed method.

2.1. Power control using the traditional Droop method

According to studies [1]–[4], the traditional Droop method for power distribution between power sources is derived from the equivalent circuit shown in Figure 2. Based on Figure 2, studies [1]-[4] have calculated the power supplied by the power source to the load as (1).

$$\tilde{S}=\dot{V}.I^{*}=\dot{V}.\left(\frac{\dot{V}-\dot{V}_{AC}}{\dot{Z}}\right)^{*}=V.e^{j\delta_1}\left(\frac{Ve^{j\delta_1}-V_{AC}e^{j\delta_2}}{Ze^{j\theta}}\right)^{*}=P+jQ \quad (1)$$

Where R and X = ωL are the resistance and reactance of a conductor; V is the voltage at the source; V_{AC} is the voltage at the end of the line; and δ is the phase angle difference between V and V_{AC}: $\delta=\delta_1-\delta_2$

$$\dot{Z}=Ze^{j\theta}=R+jX$$

The (1) can be transformed into:

$$\sin\delta=\frac{XP-RQ}{VV_{AC}} \quad (2)$$

$$V-V_{AC}\cos\delta=\frac{RP+XQ}{V} \quad (3)$$

According to studies [5]-[7], the actual angle δ is a small value, so sinδ≈δ and cosδ=1, when X >> R, from (2) and (3) can be written (4) and (5).

$$\delta=\frac{XP}{VV_{AC}} \quad (4)$$

$$V-V_{AC}=\frac{XQ}{V} \quad (5)$$

According to studies [8]-[10], from (4) and (5), the slope controllers P/f and Q/V can be set up to control the active and reactive power of the inverters as (6) and (7).

$$f=f_0-m_pP \quad (6)$$

$$V=V_0-m_qQ \quad (7)$$

m_p characterizes the slope of (6), m_q characterizes the slope of (7), and they are calculated as (8).

$$m_p=\frac{f_0-f_{min}}{P_{max}}\ ;\ m_q=\frac{V_0-V_{min}}{Q_{max}} \quad (8)$$

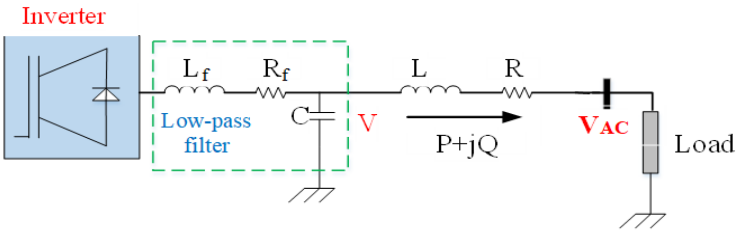

Figure 2. Equivalent circuit diagram of a power source supplying a load

2.2. Analysis of the characteristics of the traditional Dropper method

The (6) is drawn in Figure 3 (Droop P/f). It shows that if the load increases, the frequency will decrease, and if the load increases significantly, the frequency will decrease significantly. Therefore, this paper will present a method to shift the Droop P/f characteristic curve up a segment to become the Droop P/f' characteristic curve to reduce the frequency deviation from the rated value when the load increases. The content of the frequency shifting method will be presented in section 2.3.

The (7) is drawn in Figure 4 (Droop Q/V). It shows that if the load increases, the voltage will decrease, and if the load increases significantly, the voltage will decrease significantly. Therefore, this paper will present a method to shift the Droop Q/V characteristic curve up a segment to become the Droop Q/V' characteristic curve to reduce the voltage deviation from the rated value when the load increases. The content of the frequency shifting method will be presented in section 2.3. In Figure 3, V_0 and f_0 represent the rated values of voltage and frequency, respectively, while V and f denote the actual operating values. Furthermore, P_0 and Q_0 indicate the rated values of active and reactive power, respectively. Meanwhile, P and Q represent the actual active and reactive power conditions during system operation.

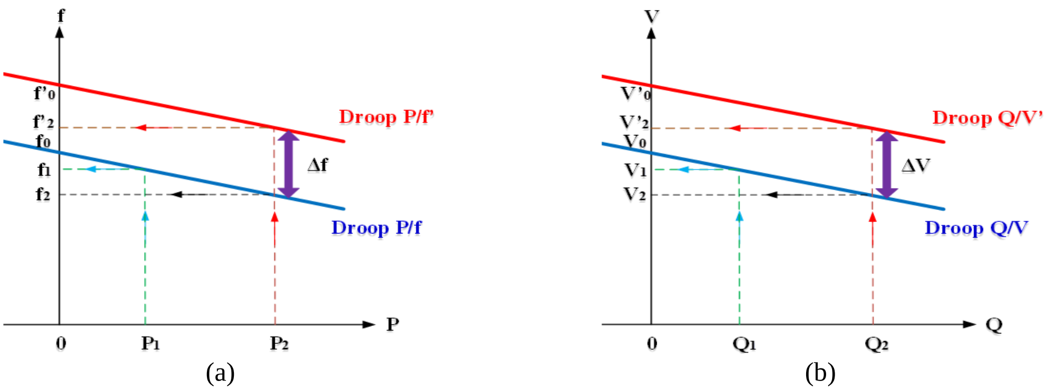

Figure 3. Droop controller characteristic curves: (a) droop P/f and (b) droop Q/V

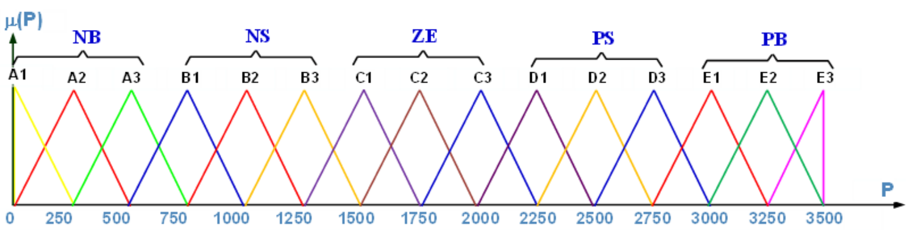

Figure 4. Membership function of input P

2.3. Proposed control method

2.3.1. Design of the fuzzy logic frequency controller

This paper aims to reduce frequency deviation when the load changes. Therefore, this paper proposes a method to shift the frequency of the P/f droop characteristic curves to maintain the stability of frequency within the allowable range using fuzzy logic. The theoretical basis of fuzzy logic is referred to in the document [16].

Specifically, fuzzy logic is used to shift the P/f graph along the f-axis by a distance Δf (the P/f' graph) in order to reduce the frequency deviation, as shown in Figure 3(a).

Figure 3(a) shows that when $P = P_1$ then $f_1 < f_0$, when the AC load increases $P = P_2$ then frequency decreases ($f_2 < f_1 < f_0$). The fuzzy controller will shift the P/f droop line up by a distance Δf. Then (6) is improved as (9).

$$f' = f_0 - m_p P + \Delta f \tag{9}$$

Where: Δf is determined by the fuzzy logic frequency block

Fuzzy logic frequency controller design: The fuzzy logic frequency controller is designed using active power (P) as the input variable and frequency deviation (Δf) as the output variable. The linguistic variables for the input and output signals are defined as shown in Figures 4 and 5, respectively. Based on the actual load power conditions, the input power domain for P is selected within the range of [0, 3500]. Meanwhile, based on the allowable frequency deviation, the output domain for Δf is selected within the range of [0, 1]. The membership functions for both input and output variables are presented in Figures 4 and 5.

The fuzzy control rules are established according to (6) and Figure 3(a). The relationship between the input power and frequency deviation is represented using a set of linguistic rules. The corresponding fuzzy rules are summarized as follows:

- If P = A1 then Δf = a1; If P = A2 then Δf = a2; If P = A3 then Δf = a3
- If P = B1 then Δf = b1; If P = B2 then Δf = b2; If P = B3 then Δf = b3
- If P = C1 then Δf = c1; If P = C2 then Δf = c2; If P = C3 then Δf = c3
- If P = D1 then Δf = d1; If P = D2 then Δf = d2; If P = D3 then Δf = d3
- If P = E1 then Δf = e1; If P = E2 then Δf = e2; If P = E3 then Δf = e3

2.3.2. Design of the fuzzy logic voltage controller

This paper aims to reduce voltage deviation when the load changes. Therefore, this paper proposes a method to shift the Q/V droop characteristic curves to maintain the stability of voltage within the allowable range using fuzzy logic. Specifically, fuzzy logic is used to shift the Q/V graph along the f-axis by a distance ΔV (the Q/V' graph) to reduce the voltage deviation, as shown in Figure 3(b). Specifically, fuzzy logic is used to shift the Q/V graph along the V-axis by a distance ΔV (the Q/V' graph) in order to reduce the voltage deviation, as shown in Figure 3(b).

Figure 3(b) shows that when $Q = Q_1$ then $V_1 < V_0$, when the AC load increases $Q = Q_2$ then voltage decreases ($V_2 < V_1 < V_0$). The fuzzy controller will shift the Q/V droop line up by a distance ΔV. Then (7) is improved as follows:

$$V' = V_0 - m_p Q + \Delta V \tag{10}$$

Where: ΔV is determined by the fuzzy logic voltage block

Design of fuzzy logic voltage block: The fuzzy logic voltage controller is designed using reactive power (Q) as the input variable and voltage deviation (ΔV) as the output variable. The linguistic variables for the input and output signals are defined as shown in Figures 6 and 7, respectively. Based on the actual load power, the input value domain for Q is selected within the range of [0, 3500]. Meanwhile, based on the allowable voltage deviation, the output value domain for ΔV is selected within the range of [0, 5]. The membership functions for both input and output variables are presented in Figures 6 and 7.

The fuzzy control rules are established according to (7) and Figure 4. The relationship between the reactive power input and voltage deviation is represented using a set of linguistic rules. The corresponding fuzzy rules are summarized as follows:

- If Q = A1 then ΔV = a1; If Q = A2 then ΔV = a2; If Q = A3 then ΔV = a3
- If Q = B1 then ΔV = b1; If Q = B2 then ΔV = b2; If Q = B3 then ΔV = b3
- If Q = C1 then ΔV = c1; If Q = C2 then ΔV = c2; If Q = C3 then ΔV = c3
- If Q = D1 then ΔV = d1; If Q = D2 then ΔV = d2; If Q = D3 then ΔV = d3
- If Q = E1 then ΔV = e1; If Q = E2 then ΔV = e2; If Q = E3 then ΔV = e3

Use the Sum-Product principle and the centroid method to defuzzify.

The block diagram of the proposed controller is shown in Figure 8. The proposed controller includes a droop improvement block using fuzzy logic to shift frequency and voltage according to (9) and (10). In order to improve the sustainability and stability of the proposed controller during voltage and frequency shifting, this paper uses a Sliding mode controller to control the output voltage and current of the inverter.

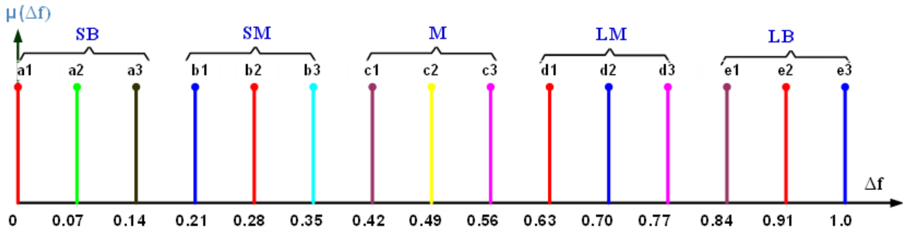

Figure 5. Membership function of output Δf

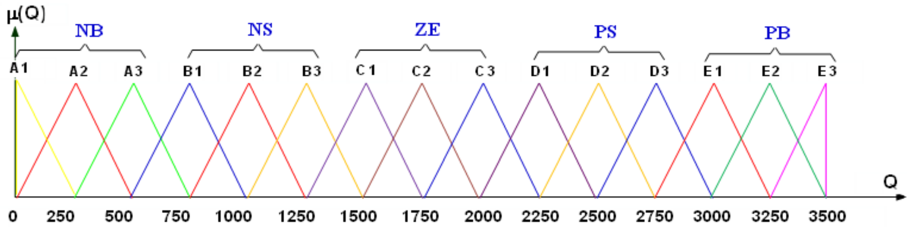

Figure 6. Membership function of input Q

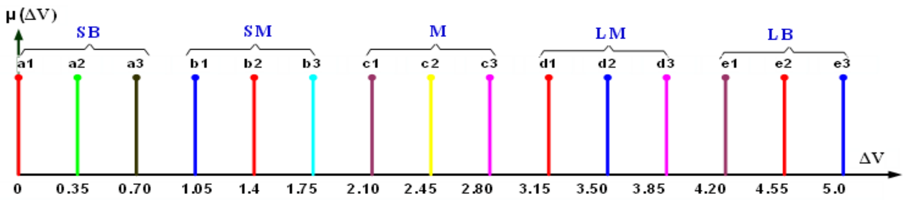

Figure 7. Membership function of output ΔV

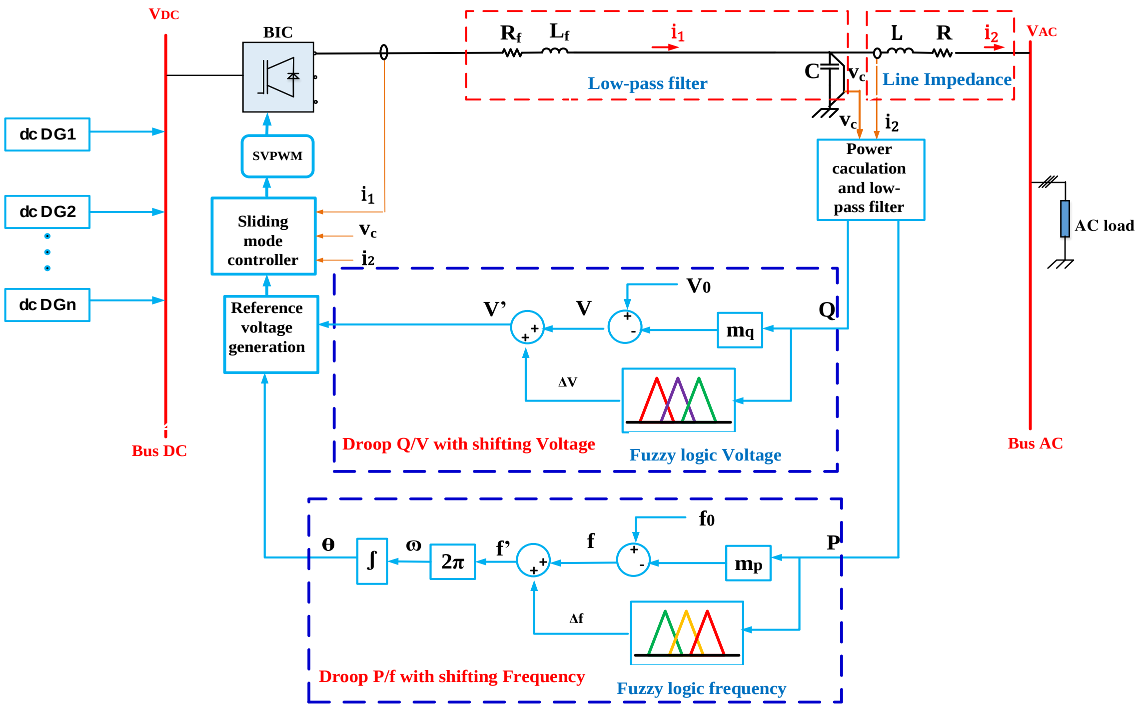

Figure 8. Block diagram of the proposed controller for an inverter in an islanded microgrid

2.3.3. Design of the sliding mode controller

Using a sliding mode controller (SMC) to improve the robustness and stability of the system during voltage and frequency shifts, the SMC is presented as follows: The purpose of the SMC is to make the signals at the inverter output closely track the reference value of the inverter input. The theoretical basis of the SMC is referenced in studies [24], [25]. From Figure 9, we have (11).

$$\begin{aligned} \frac{dv_c}{dt} &= \frac{1}{C}i_1 - \frac{1}{C}i_2 \\ \frac{di_1}{dt} &= \frac{1}{L_f}v_{inv} - \frac{1}{L_f}v_c - \frac{R_f}{L_f}i_1 \\ \frac{di_2}{dt} &= \frac{1}{L}v_c - \frac{1}{L}v_{pcc} - \frac{R}{L}i_2 \end{aligned} \tag{11}$$

Transforming system (11) to the dq0 coordinate system, we have the following systems (12) and (13).

$$\begin{aligned} \dot{v}_{Cd} &= \frac{1}{C}i_{1d} - \frac{1}{C}i_{2d} + \omega v_{cq} \\ \dot{i}_{1d} &= \frac{v_{invd}}{L_f} - \frac{1}{L_f}v_{cd} - \frac{R_f}{L_f}i_{1d} + \omega i_{1q} \\ \dot{i}_{2d} &= \frac{v_{cd}}{L} - \frac{1}{L}v_{pccd} - \frac{R}{L}i_{2d} + \omega i_{2q} \end{aligned} \tag{12}$$

$$\begin{aligned} \dot{v}_{Cq} &= \frac{1}{C}i_{1q} - \frac{1}{C}i_{2q} - \omega v_{cd} \\ \dot{i}_{1q} &= \frac{v_{invq}}{L_f} - \frac{1}{L_f}v_{cq} - \frac{R_f}{L_f}i_{1q} - \omega i_{1d} \\ \dot{i}_{2q} &= \frac{v_{cq}}{L} - \frac{1}{L}v_{pccq} - \frac{R}{L}i_{2q} - \omega i_{2d} \end{aligned} \tag{13}$$

The purpose of the SMC is to ensure that the voltage V_C closely follows V_{ref}, so we define the deviations:

$$\begin{aligned} e_d &= v_{Cd} - v_{Cd}^* \\ e_q &= v_{Cq} - v_{Cq}^* \end{aligned} \tag{14}$$

Where: $v_{Cd}^* = v_{refd}$; $v_{Cq}^* = v_{refq}$. Choose the sliding surfaces for (14):

$$\begin{aligned} S_d &= \dot{e}_d + a\,e_d = (\dot{v}_{Cd} - \dot{v}_{Cd}^*) + a(v_{Cd} - v_{Cd}^*) \\ S_q &= \dot{e}_q + a\,e_q = (\dot{v}_{Cq} - \dot{v}_{Cq}^*) + a(v_{Cq} - v_{Cq}^*) \end{aligned} \tag{15}$$

$$\begin{aligned} \dot{S}_d &= \ddot{e}_d + a\dot{e}_d = (\ddot{v}_{Cd} - \ddot{v}_{Cd}^*) + a(\dot{v}_{Cd} - \dot{v}_{Cd}^*) \\ \dot{S}_q &= \ddot{e}_q + a\dot{e}_q = (\ddot{v}_{Cq} - \ddot{v}_{Cq}^*) + a(\dot{v}_{Cq} - \dot{v}_{Cq}^*) \end{aligned} \tag{16}$$

Where: a = constant; a > 0. Using the Lyapunov stability principle: $V_d = \frac{1}{2}S_d^2$. Therefore, we choose:

$$\begin{aligned} \dot{S}_d &= -k\,\mathrm{sign}(S_d) \\ \dot{S}_q &= -k\,\mathrm{sign}(S_q) \end{aligned} \tag{17}$$

Where: k= constant; k>0. From the systems of (12) to (17), we can derive (18) and (19).

$$u_d = v_{invd} = CL_f\Big[-k\,\mathrm{sign}(S_d) + Ai_{1d} + Bv_{Cd} + Di_{2d} + \frac{2\omega}{C}i_{2q} - \frac{2\omega}{C}i_{1q} - \omega a v_{Cq} + \ddot{v}_{Cd}^* - \frac{1}{CL}v_{pccd} + a\dot{v}_{Cd}^*\Big] \tag{18}$$

$$u_q = v_{invq} = CL_f\Big[-k\,\mathrm{sign}(S_q) + Ai_{1q} + Bv_{Cq} + Di_{2q} - \frac{2\omega}{C}i_{2d} + \frac{2\omega}{C}i_{1d} + \omega a v_{Cd} + \ddot{v}_{Cq}^* - \frac{1}{CL}v_{pccq} + a\dot{v}_{Cq}^*\Big] \tag{19}$$

Where:

$$A=\left(\frac{R_f}{CL_f}-\frac{a}{C}\right);\ B=\left(\frac{1}{CL_f}+\frac{1}{CL}+\omega^2\right);\ D=\left(\frac{a}{C}-\frac{R}{LC}\right)$$

The sliding mode controller is implemented according to (18) and (19). In which v^*_{Cd} and v^*_{Cq} are reference voltages, u is the inverter control signal, which is the voltage signal to modulate the inverter.

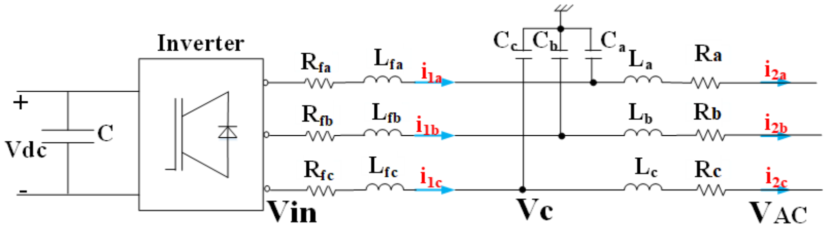

Figure 9. Equivalent schematic of an inverter connected to load

3. RESULTS AND DISCUSSION

Perform a simulation for the microgrid configured as shown in Figure 1, which consists of 3 inverters connected in parallel. Use both controllers: the conventional controller and the proposed controller. The data used for the simulation are given in Table 1.

Table 1. Data used for simulation

Parameters name	Value	Parameters name	Value
DC link voltage V_{cd} (V)	600	f_0 (Hz)	50
		f_{max} (Hz)	51
		f_{min} (Hz)	49.5
L_f (mH)	4.2	S(kVA)	4
R_f (Ω)	0.1	$V_{AC,0}$ (V)	311
		$V_{AC,max}$ (V)	315
		$V_{AC,min}$ (V)	305
C (μF)	2.2	Sope coefficient m_q (V/Var)	0.000105
f_z (kHz)	5	Sope coefficient m_p (rad/s /W)	0.0001
Line impedance parameters			
L (H)	0.003	R (Ω)	1

3.1. Case 1

Power sharing simulation for a standalone microgrid with two inverters connected in parallel, the simulation is performed using the proposed controller and the conventional controller. The two inverters are assumed to have the same rated power P_{1dm}: P_{2dm} = 1:1. At time t = 10 s, the power consumption of the load increases. The simulation results are presented in Figures 10 and 11.

The proposed controller gives the result of dividing active power and reactive power exactly in the ratio of 1:1, as shown in Figures 10(a) and 10(b). The settling time is relatively early, and the response is stable even when the load changes sharply. Figures 11(a) and 11(b) show that the conventional controller gives less accurate power division results than the proposed controller, and worse stability than the proposed controller during the period of strong load changes.

Figures 10(c) and 11(c) are the single-phase currents of inverters 1 and 2. Figure 10(c) shows that the two waveforms match exactly, while Figure 11(c) shows that the two waveforms have different amplitudes during the load change period. Figures 10(d) and 11(d) are voltage at the load. In the period from 0s to 10s, the reactive power output of each inverter is $Q_1 = Q_2 = 990$ Var, so according to Figures 6 and 7, the Q/V droop line will shift up a distance of ΔV=1.4(V) along the vertical axis, the Q/V droop line becomes the Q/V' droop line as in Figure 3(b) or (10), so the AC bus voltage of the proposed method (309.5 V) is raised higher than the traditional method (307 V). The ΔV shift of the Q/V droop depends on the value domain of the output of the fuzzy logic set selected above. In the period from 10s to 20s, the reactive power output of each inverter is $Q_1 = Q_2 = 1910$ Var, so according to Figures 6 and 7, the Q/V droop line will shift up a distance of ΔV=2.8 (V) along the vertical axis, the Q/V droop line becomes the Q/V' droop line as in Figure 3(b) or (10), so the AC bus voltage of the proposed method (308.3 V) is raised higher than the traditional method (300 V). The ΔV shift of the Q/V droop depends on the value domain of the output of the fuzzy logic set selected above. These results are in full agreement with the established fuzzy control law, consistent with (10). This result is in complete agreement with Figure 3(b), the AC bus voltage will decrease sharply to below the allowable level. Therefore, the proposed controller will shift the traditional droop line upward, aiming to restore the AC bus voltage, improving the power quality of the microgrid.

Figures 10(e) and 11(e) show the frequency in the microgrid. In the period from 0s to 10s, inverter output power is $P_1 = P_2 = 1380$ W, so according to Figures 4 and 5, the P/f droop line will shift up a distance of $\Delta f = 0.35$ Hz along the vertical axis, the P/f droop line becomes the P/f' droop line as in Figure 3(a) or (9), so the in the microgrid of the proposed method (50.2 Hz) is raised higher than the traditional method (49.8 Hz). The Δf shift of the P/f droop depends on the value domain of the output of the fuzzy logic set selected above. In the period from 10 s to 20 s, $P_1 = P_2 = 2765$ W, so according to Figures 4 and 5, the P/f droop line will shift up a distance of $\Delta f = 0.7$ Hz along the vertical axis, the P/f droop line becomes the P/f' droop line as in Figure 3(a) or (9), so the frequency of the proposed method (50.4 Hz) is raised higher than the traditional method (49.5 Hz). The Δf shift of the P/f droop depends on the value domain of the output of the fuzzy logic set selected above. These results are in full agreement with the established fuzzy control law, consistent with (9) and the droop line in Figure 3. Figure 3 shows that when the load increases, the frequency of the microgrid will decrease, and when the load increases sharply, the frequency will decrease sharply to below the allowable level. Therefore, the proposed controller will shift the traditional droop line upward, aiming to restore the frequency of the microgrid.

The characteristics of the proposed controller are stable and sustainable even when the load changes sharply, the SMC controller makes the current and voltage signals at the inverter output lie on the designed sliding surface S. This shows that the combination of the Sliding mode controller and the improved droop controller has performed accurate power division in the case of a sharp increase in load, improving the power quality and dynamic response of the microgrid, the current, voltage and power characteristics are very stable. The results of evaluating the ability to eliminate circulating current between inverters during operation, assessed by the power division deviation between them and the voltage and frequency stability in the microgrid, are presented in Table 2.

Thus, the proposed controller successfully controls voltage and frequency oscillations within acceptable ranges, with very small deviations from the rated values. In addition, it is capable of precise power division. As a result, the circulating current between the inverters is eliminated.

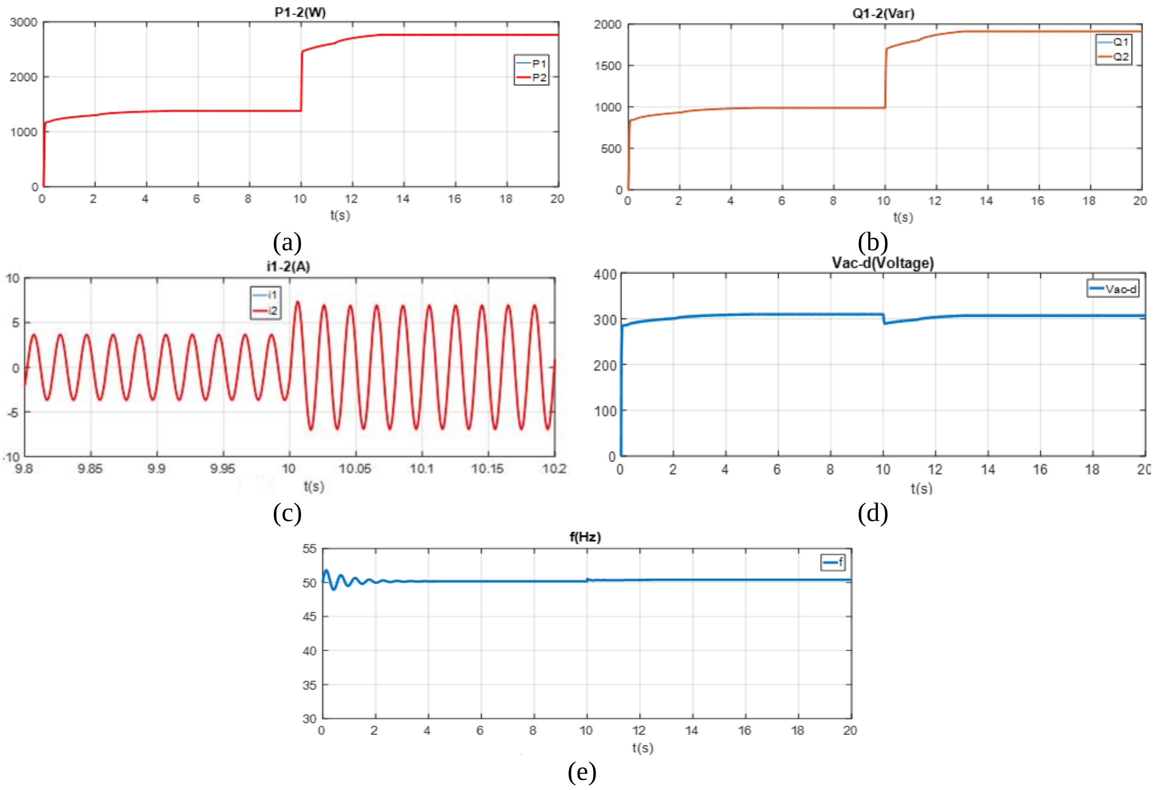

Figure 10. The simulation results with the proposed controller: (a) active power, (b) reactive power, (c) current, (d) voltage, and (e) frequency

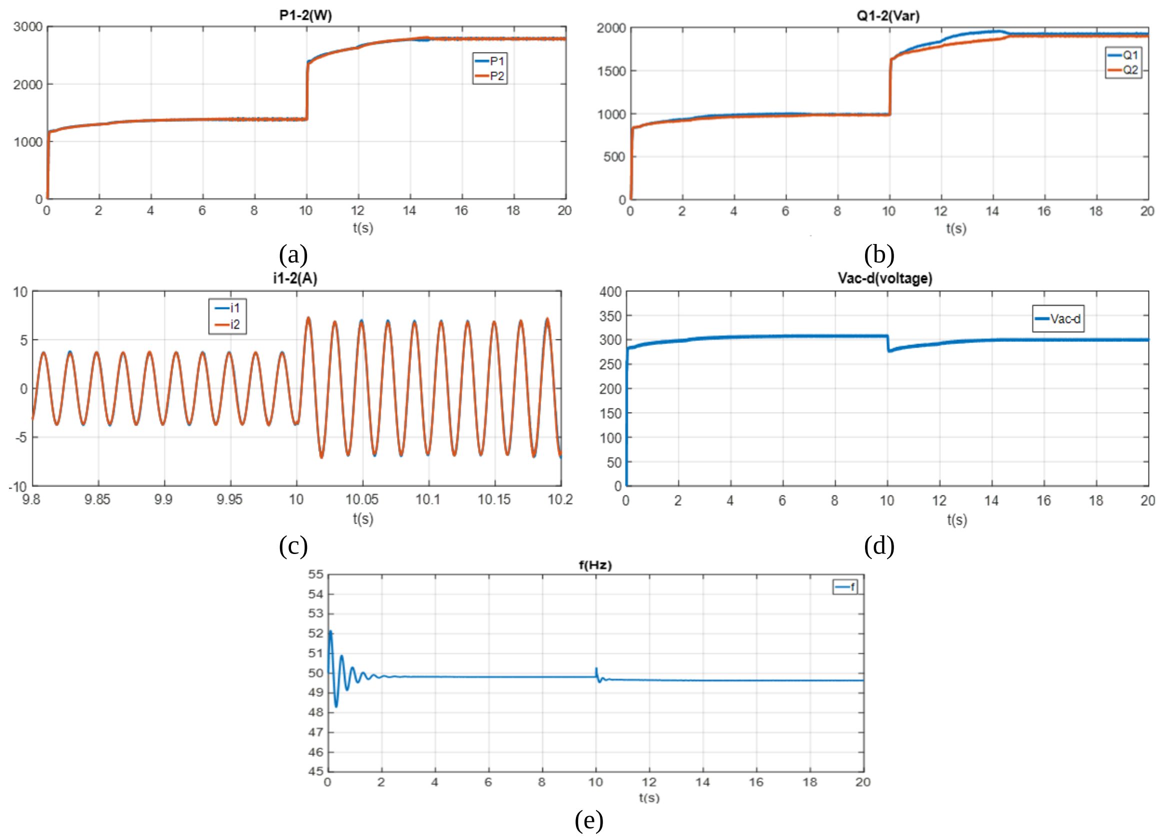

Figure 11. The simulation results with the conventional controller: (a) active power, (b) reactive power, (c) current, (d) voltage, (e) frequency

Table 2. Evaluate the results regarding voltage, frequency, and power deviations

Simulation time (seconds)	Value	
Controller	0–10 s	10–20 s
Proposed controller	$P_1 = P_2 = 1380$ W $Q_1 = Q_2 = 990$ Var $\Delta V = V_0 - V = 311 - 309.5 = 1.5$ V $\Delta f = f_0 - f = 50 - 50.2 = 0.2$ Hz	$P_1 = P_2 = 2765$ W $Q_1 = Q_2 = 1910$ Var $\Delta V = V_0 - V = 311 - 308.3 = 2.7$ V $\Delta f = f_0 - f = 50 - 50.4 = -0.4$ Hz
Conventional controller	$P_1 = P_2 = 1380$ W $Q_1 = 1000$ Var $Q_2 = 980$ Var $\Delta V = V_0 - V = 311 - 307 = 4$ V $\Delta f = f_0 - f = 50 - 49.8 = 0.2$ Hz	$P_1 = P_2 = 2765$ W $Q_1 = 1930$ Var $Q_2 = 1890$ Var Unstable curve for about 10-14 seconds $\Delta V = V_0 - V = 311 - 300 = 11$ V $\Delta f = f_0 - f = 50 - 49.5 = 0.5$ Hz

3.2. Case 2

Simulate a microgrid with three inverters of equal power (Pđm1 = Pđm2 = Pđm3) using the proposed controller. The proposed controller gives the result of dividing exactly in the ratio of 1:1:1, as shown in Figures 12(a) and 12(b). The settling time is relatively early, and the response is stable even when the load changes sharply. Figure 12(c) shows the single-phase currents of inverters 1 and 2. Figure 12(c) shows that the two waveforms match exactly, and Figure 12(d) is voltage at the load. In the period from 0 s to 10 s, the reactive power output of each inverter is $Q_3 = Q_1 = Q_2 = 990$ Var, so according to Figures 6 and 7, the graph Q/V will shift up a distance of ΔV=1.4 (V) along the vertical axis, the graph Q/V becomes the graph Q/V' as in Figure 3(b) or (10), so the voltage at load is 309.5 V. The ΔV shift of the Q/V droop depends on the value domain of the output of the fuzzy logic set selected above. In the period from 10 s to 20 s, the reactive power output of each inverter is $Q_1 = Q_2 = Q_3 = 1900$ Var, so according to Figures 6 and 7, the graph Q/V will shift up a distance of ΔV = 2.8 (V) along the vertical axis, the Q/V droop line becomes the graph Q/V' droop as in Figure 3(b) or (10), so the AC bus voltage is 308 V. The ΔV shift of the graph Q/V depends on the value domain of the output of the fuzzy logic set selected above. These results are in full agreement with the established fuzzy control law, consistent with (10) and the graph droop in Figure 3(b). Therefore, the proposed controller will shift the traditional droop line upward, aiming to restore voltage at the load, improving the power quality of the microgrid. Figure 12(e) is the frequency in the microgrid. In the period from 0 s to 10 s as $P_1 = P_2 = P_1$ =1347 W, so according to Figures 4 and 5, the graph droop P/f will shift up a distance of Δf = 0.33 (Hz) along the vertical axis, the graph droop/f becomes the graph droop P/f' as in Figure 3 or (9), so the in the microgrid is 50.2 Hz. The Δf shift of the graph droop P/f depends on the value domain of the output of the fuzzy logic set selected above. In the period from 10 s to 20 s, as $P_1 = P_2$ = 2581 W, so according to Figures 4 and 5, the graph droop P/f will shift up a distance of Δf = 0.65 Hz along the vertical axis, the graph droop P/f becomes the graph droop P/f' as in Figure 3 or (9), so the frequency of the proposed method is 50.3 Hz. The Δf shift of the graph droop P/f depends on the value domain of the output of the fuzzy logic set selected above. These results are in full agreement with the established fuzzy control law, consistent with (9). Therefore, the proposed controller will shift the traditional droop line upward, aiming to restore the frequency of the microgrid. The combination of SMC makes the proposed controller stable and robust even when the load changes suddenly.

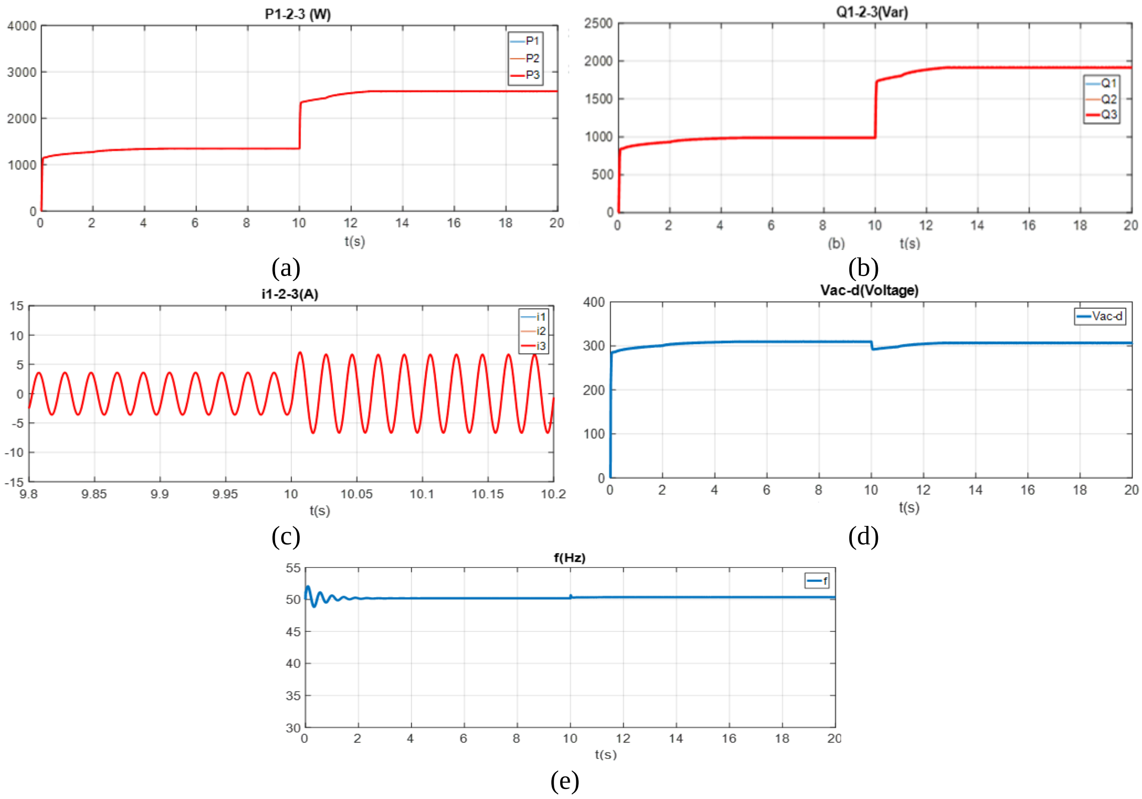

Figure 12. The simulation results with the proposed controller ($P_{đm1}$: $P_{đm2}$: $P_{đm3}$ =1:1:1):
(a) active power, (b) reactive power, (c) current, (d) voltage, and (e) frequency

4. CONCLUSION

By combining fuzzy logic and SMC, the proposed method achieves absolutely precise power distribution for parallel-connected inverters in a microgrid, eliminating balancing currents between inverters. Furthermore, the proposed method can improve the power quality supplied to loads in the microgrid. Moreover, the control system remains stable even with sudden load changes. In the future, this method will be applied to microgrids comprising multiple AC subgrids, multiple DC subgrids, DC loads, and AC loads.

FUNDING INFORMATION

This research did not receive any funding.

AUTHOR CONTRIBUTIONS STATEMENT

This journal uses the Contributor Roles Taxonomy (CRediT) to recognize individual author contributions, reduce authorship disputes, and facilitate collaboration.

Name of Author	C	M	So	Va	Fo	I	R	D	O	E	Vi	Su	P	Fu
Xuan Hoa Thi Pham	✓	✓	✓		✓		✓	✓	✓	✓			✓	
Hai Van Tran	✓			✓		✓				✓	✓	✓	✓	

C : **C**onceptualization
M : **M**ethodology
So : **So**ftware
Va : **Va**lidation
Fo : **Fo**rmal analysis
I : **I**nvestigation
R : **R**esources
D : **D**ata Curation
O : Writing - **O**riginal Draft
E : Writing - Review & **E**diting
Vi : **Vi**sualization
Su : **Su**pervision
P : **P**roject administration
Fu : **Fu**nding acquisition

CONFLICT OF INTEREST STATEMENT

The author states no conflict of interest with respect to the research, authorship, and publication of the article.

DATA AVAILABILITY

The data supporting the findings of this study are available upon request from the corresponding authors.

REFERENCES

[1] F. Bao, J. Guo, W. Wang, and B. Wang, "Cooperative control strategy of multiple VSGs in microgrid based on adjacent information," *IEEE Access*, vol. 9, pp. 125603–125615, 2021, doi: 10.1109/ACCESS.2021.3110848.

[2] V. Gurugubelli, A. Ghosh, A. K. Panda, and S. Rudra, "Implementation and comparison of droop control, virtual synchronous machine, and virtual oscillator control for parallel inverters in standalone microgrid," *International Transactions on Electrical Energy Systems*, vol. 31, no. 5, May 2021, doi: 10.1002/2050-7038.12859.

[3] A. Rosini, A. Labella, A. Bonfiglio, R. Procopio, and J. M. Guerrero, "A review of reactive power sharing control techniques for islanded microgrids," *Renewable and Sustainable Energy Reviews*, vol. 141, p. 110745, May 2021, doi: 10.1016/j.rser.2021.110745.

[4] Y. Guan, W. Feng, J. Lu, J. M. Guerrero, and J. C. Vasquez, "A novel grid-connected harmonic current suppression control for autonomous current sharing controller-based AC microgrids," in *2018 IEEE Energy Conversion Congress and Exposition (ECCE)*, Sep. 2018, pp. 5899–5904. doi: 10.1109/ECCE.2018.8557795.

[5] X. Liu and R. Gong, "A control strategy of microgrid-connected system based on VSG," in *2020 IEEE International Conference on Power, Intelligent Computing and Systems (ICPICS)*, Jul. 2020, pp. 739–743. doi: 10.1109/ICPICS50287.2020.9201955.

[6] R. Nandi, M. Tripathy, C. P. Gupta, "Adaptive virtual impedance based dual mode inverter controller for power and voltage coordination in LV AC microgrid," *IEEE Transactions on Industry Applications*,Vol. 60, no. 6, 2024, pp. 8495 – 8508, doi: 10.1109/TIA.2024.3443777.

[7] M. W. Khan, G. Li, K. Wang, M. Numan, L. Xiong, and M. A. Khan, "Optimal control and communication strategies in multi-energy generation grid," *IEEE Communications Surveys & Tutorials*, vol. 25, no. 4, pp. 2599–2653, 2023, doi: 10.1109/COMST.2023.3304982.

[8] G. Vikash and A. Ghosh, "Parallel inverters control in standalone microgrid using different droop control methodologies and virtual oscillator control," *Journal of The Institution of Engineers (India): Series B*, vol. 103, no. 1, pp. 163–171, Feb. 2022, doi: 10.1007/s40031-021-00613-6.

[9] B. Zhang, B. Liu, F. Zheng, B. Yu, Q. Yu, "A dual-frequency-droop based nonactive power sharing control method for ac microgrids," *IEEE 16th International Symposium on Power Electronics for Distributed Generation Systems (PEDG)*, doi: 10.1109/PEDG62294.2025.11060197.

[10] S. Tiwari, "An intelligent protection scheme based on support vector machine for fault detection in microgrid using transient signals in protection scheme," *Serbian Journal of Electrical Engineering*, vol. 21, no. 3, pp. 327–343, 2024, doi: 10.2298/SJEE2403327T.

[11] S. P. Tiwari, "An efficient protection scheme for critical fault detection in microgrid under uncertain scenarios using deep learning algorithm," *Electrical Engineering*, vol. 107, no. 7, pp. 9009–9023, Jul. 2025, doi: 10.1007/s00202-024-02861-3.

[12] S. P. Tiwari, "An adaptive and reliable protection scheme for critical fault detection in IEC microgrid considering dissimilar AC faults and weather-based random scenarios," *Electrical Engineering*, vol. 106, no. 5, pp. 6373–6387, 2024, doi: 10.1007/s00202-024-02386-9.

[13] S. P. Tiwari, "A protection scheme based on ensemble of linear discriminant analysis for fault detection in microgrid considering varying operational conditions," *Multimedia Tools and Applications*, vol. 84, no. 18, pp. 20269–20287, Jul. 2024, doi: 10.1007/s11042-024-19871-9.

[14] B. Maroua, Z. Laid, H. Benbouhenni, M. Fateh, N. Debdouche, and I. Colak, "Robust type 2 fuzzy logic control microgrid-connected photovoltaic system with battery energy storage through multi-functional voltage source inverter using direct power control," *Energy Reports*, vol. 11, pp. 3117–3134, Jun. 2024, doi: 10.1016/j.egyr.2024.02.047.

[15] H. Assem, T. Azib, F. Bouchafaa, C. Laarouci, N. Belhaouas, and A. Hadj Arab, "Adaptive fuzzy logic-based control and management of photovoltaic systems with battery storage," *International Transactions on Electrical Energy Systems*, vol. 2023, pp. 1–18, May 2023, doi: 10.1155/2023/9065061.

[16] O. Feddaoui, R. Toufouti, L. Jamel, and S. Meziane, "Fuzzy logic control of hybrid systems including renewable energy in microgrids," *International Journal of Electrical and Computer Engineering*, vol. 10, no. 6, pp. 5559–5569, 2020, doi: 10.11591/ijece.v10i6.pp5559-5569.

[17] X. H. T. Pham, "Improved power controller for enhancement of voltage quality in microgrid," *The Journal of Engineering*, vol. 2022, no. 8, pp. 773–787, Aug. 2022, doi: 10.1049/tje2.12147.

[18] K. A. Al Sumarmad, N. Sulaiman, N. I. A. Wahab, and H. Hizam, "Microgrid energy management system based on fuzzy logic and monitoring platform for data analysis," *Energies*, vol. 15, no. 11, p. 4125, Jun. 2022, doi: 10.3390/en15114125.
[19] K. T. Nguyen, G. W. Chang, and W.-Y. Huang, "A practical method for inverter output power sharing with harmonic voltage control in islanded microgrid," in *2024 IEEE Power & Energy Society General Meeting (PESGM)*, IEEE, Jul. 2024, pp. 1–5. doi: 10.1109/PESGM51994.2024.10688766.
[20] S. Sen, S. S. Rangarajan, C. K. Shiva, B. Vedik, R. Kumar, and S. N, "Controller design for hybrid AC/DC microgrid system with renewable sources and motor loads," in *2023 Third International Conference on Advances in Electrical, Computing, Communication and Sustainable Technologies (ICAECT)*, Jan. 2023, pp. 1–6. doi: 10.1109/ICAECT57570.2023.10117722.
[21] M. Wu, D. Miao, C. Huang, and W. Si, "Research on the power sharing strategy of islanded hybrid AC/DC microgrid under master-slave control," in *2024 4th Power System and Green Energy Conference (PSGEC)*, Aug. 2024, pp. 1158–1162. doi: 10.1109/PSGEC62376.2024.10721084.
[22] K. Zhang, M. Su, Z. Liu, H. Han, X. Zhang, and P. Wang, "A distributed coordination control for islanded hybrid AC/DC microgrid," *IEEE Systems Journal*, vol. 17, no. 2, pp. 1819–1830, Jun. 2023, doi: 10.1109/JSYST.2023.3242119.
[23] X. Ge, X. Zhang, X. Jin, H. Ma, J. Tian, and R. Li, "A novel decentralized control for cascaded-type AC microgrids operating in grid-connected and islanded modes," in *2022 4th International Conference on Smart Power & Internet Energy Systems (SPIES)*, Dec. 2022, pp. 1451–1457. doi: 10.1109/SPIES55999.2022.10082495.
[24] M. J. Najafirad, N. M. Dehkordi, and H. Nazaripouya, "Voltage control of islanded DC microgrid using hierarchical controllers based on kharitonov theory," in *2023 IEEE Power & Energy Society General Meeting (PESGM)*, Jul. 2023, pp. 1–5. doi: 10.1109/PESGM52003.2023.10253356.
[25] D. Truong, X. H. T. Pham, N. X. Doan, and H. Van Tran, "Power control in microgrid using improved virtual impedance method," *The Journal of Engineering*, vol. 2023, no. 5, May 2023, doi: 10.1049/tje2.12274.

BIOGRAPHIES OF AUTHORS

Xuan Hoa Thi Pham received her M.S. and Ph.D. degrees from the Ho Chi Minh City University of Technology, Ho Chi Minh City, Vietnam, in 2006 and 2018, respectively. She has been working as a lecturer of electrical and electronic engineering at the Ho Chi Minh City University of Industry and Trade, Ho Chi Minh City, Vietnam, since 2002. Her current research interests include renewable energy interfaces, microgrids, and power quality. She can be contacted at email: hoaptx@huit.edu.vn.

Hai Van Tran finished a bachelor's degree and a master's degree in electrical engineering from HCMC University of Technology and Education, Vietnam, in 2007 and 2009, respectively. Now, he is working at the Faculty of Electrical and Electronic Technology, Ho Chi Minh City University of Industry and Trade (HUIT), Vietnam. His research fields are transmission power networks, optimization control, and new energies such as wind and photovoltaic. He can be contacted at email: haitv@huit.edu.vn.